Nanostructured Reduced Graphene Oxide/Fe_2O_3 Composite As a High-Performance Anode Material for Lithium Ion Batteries

Xianjun Zhu,[†,‡] Yanwu Zhu,[‡] Shanthi Murali,[‡] Meryl D. Stoller,[‡] and Rodney S. Ruoff[‡,*]

[†]College of Chemistry, Central China Normal University, 152 Luoyu Road, Hubei, Wuhan 430079, People's Republic of China, and [‡]Department of Mechanical Engineering and the Texas Materials Institute, The University of Texas at Austin, Austin, Texas 78712, United States

ABSTRACT Reduced graphene oxide/Fe_2O_3 composite was prepared using a facile two-step synthesis by homogeneous precipitation and subsequent reduction of the G-O with hydrazine under microwave irradiation to yield reduced graphene oxide (RG-O) platelets decorated with Fe_2O_3 nanoparticles. As an anode material for Li-ion batteries, the RG-O/Fe_2O_3 composite exhibited discharge and charge capacities of 1693 and 1227 mAh/g, respectively, normalized to the mass of Fe_2O_3 in the composite (and ~1355 and 982 mAh/g, respectively, based on the total mass of the composite), with good cycling performance and rate capability. Characterization shows that the Fe_2O_3 nanoparticles are uniformly distributed on the surface of the RG-O platelets in the composite. The total specific capacity of RG-O/Fe_2O_3 is higher than the sum of pure RG-O and nanoparticle Fe_2O_3, indicating a positive synergistic effect of RG-O and Fe_2O_3 on the improvement of electrochemical performance. The synthesis approach presents a promising route for a large-scale production of RG-O platelet/metal oxide nanoparticle composites as electrode materials for Li-ion batteries.

KEYWORDS: reduced graphene oxide · Fe_2O_3 · anode · lithium ion battery · homogeneous precipitation

Rechargeable Li-ion batteries are considered as the leading candidates for hybrid, plug-in hybrid, and all electronic vehicles. Graphite has been employed as standard anode material in Li-ion batteries because lithium can be inserted/deinserted during discharging and charging, resulting in a theoretical specific capacity of 372 mAh/g.[1] In order to meet the increasing demand for higher energy density batteries, it is essential to develop electrodes made from durable, nontoxic, and inexpensive materials with a high charge/discharge rate and a high reversible capacity. Transition metal oxides such as Co_3O_4, MoO_3, and Fe_3O_4 are capable of Li^+ insertion/extraction in excess of 6 Li^+ per formula unit,[2−5] resulting in a significantly larger reversible capacity than that of commercial graphite. During cycling of Li^+ insertion/deinsertion, transition metal oxides typically break into small metal clusters because they can react with Li to form Li_2O, leading to a large volume expansion and a destruction of the structure upon electrochemical cycling, especially at high rates, thus resulting in severe loss of capacity with cycling and a poor electrical conductivity.[6,7]

Nanostructured metal oxide electrode materials have been used to improve the reversible capacity and rate capacity, which can be attributed to shortened Li^+ insertion/extraction pathways.[6,8] Various carbon additives have also been mixed with the metal oxide particles to improve their conductivity.[9] Among the metal oxides used for Li-ion batteries, Fe_2O_3 is an abundant, low cost, and nontoxic material and is therefore considered as one of the most promising candidate materials.[10,11] On the other hand, graphene has an excellent electronic conductivity, a high theoretical surface area of 2630 m^2/g, and excellent mechanical properties and, thus, is a promising component for high-performance electrode materials.[12−15] Recently, chemically modified graphene materials have been used to form hybrid materials with SnO_2, TiO_2, and Mn_3O_4 in attempts to improve electrode capacity and cycling stability.[16−18] However, to our best knowledge, an anode combining Fe_2O_3 with graphene-based materials for Li^+ batteries has not been reported.

Herein, we report a facile two-step synthesis of a "graphene"-Fe_2O_3 composite by homogeneous precipitation of $FeCl_3$ in a suspension of graphene oxide (G-O) platelets with urea, with subsequent reduction of the G-O with hydrazine under microwave irradiation to yield reduced graphene oxide (RG-O) platelets decorated with Fe_2O_3 nanoparticles. As an anode material for Li-ion batteries, the RG-O/Fe_2O_3 composite exhibited discharge and charge capacities of

* Address correspondence to r.ruoff@mail.utexas.edu.

Received for review February 7, 2011 and accepted March 28, 2011.

Published online March 28, 2011
10.1021/nn200493r

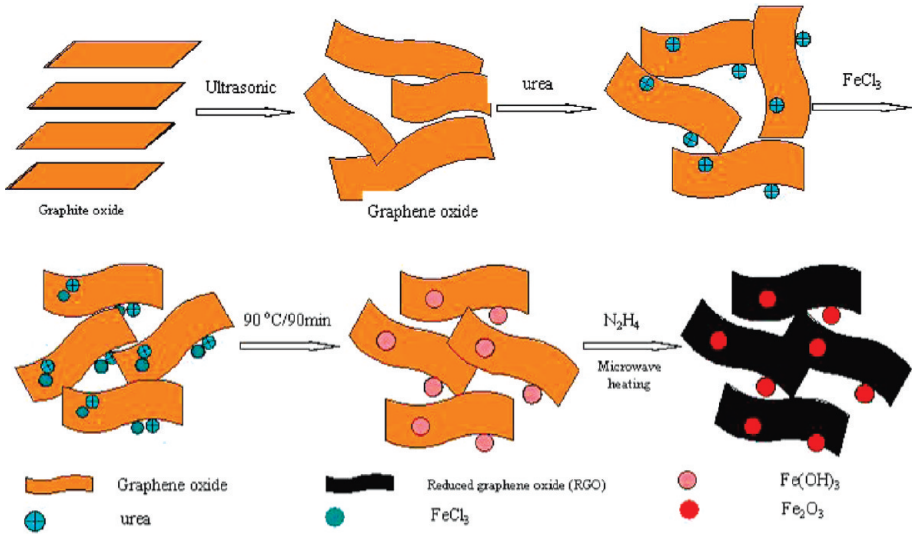

Scheme 1. Scheme of RG-O/Fe_2O_3 composite forming mechanism.

1693 and 1227 mAh/g, respectively, normalized to the mass of Fe_2O_3 in the composite (and ~1355 and 982 mAh/g, respectively, based on the total mass of the composite). In addition, the composite shows good cycling performance and rate capability. Characterization shows that the Fe_2O_3 nanoparticles are uniformly distributed on the surface of the RG-O platelets in the composite. To our best knowledge, this is the highest reported capacity for Fe_2O_3-based anode materials used in Li-ion batteries. The synthesis approach presents a promising route for a large-scale production of RG-O platelet/metal oxide nanoparticle composites as electrode materials for Li-ion batteries.

RESULTS AND DISCUSSION

As shown in Scheme 1, graphite oxide prepared by a modified Hummer method[19,20] was sonicated in water to form a suspension of G-O platelets. For the synthesis of the RG-O/Fe_2O_3 composite, $FeCl_3$ was hydrolyzed in the graphene oxide suspension in the presence of urea at 90 °C. The molar ratio of $FeCl_3$ to urea was 1:30. This step afforded a uniform $Fe(OH)_3$ coating on the surface of the graphene oxide platelets. During hydrolysis, urea releases hydroxyl ions slowly and uniformly in the suspension, resulting in the formation of $Fe(OH)_3$, as suggested by the following reactions:

$$CO(NH_2)_2 + 3H_2O \rightarrow 2NH_4^+ + CO_2 + 2OH^-$$
$$Fe^{3+} + 3OH^- \rightarrow Fe(OH)_3$$

The $Fe(OH)_3$ particles produced anchor onto the surface of the G-O platelets through oxygen-containing functional groups, such as carboxyl, hydroxyl, and epoxyl.

After the suspension was cooled to room temperature, a trace of hydrazine was added to the suspension under continuous stirring and the suspension was then irradiated with microwaves using a commercial microwave oven. During this process, G-O is converted into RG-O and $Fe(OH)_3$ decomposes to Fe_2O_3 nanoparticles as $2Fe(OH)_3 \rightarrow Fe_2O_3 + 3H_2O$. The composite obtained was characterized by XRD, which agrees well with JCPDS 97-002-2505 (see FS1 (a, b)). The XPS pattern indicates that the levels of $Fe2p_{3/2}$ and $Fe2p_{1/2}$ are, respectively, 710.56 and 724.26 eV, with the satellite peak at ~719 eV (indicated by an arrow), which is the characteristic of Fe_2O_3 (see FS1 (c)).[21] The Raman spectrum has the characteristic peaks of free Fe_2O_3 and the D and G peaks of RG-O (see FS2). It contained 20 wt % RG-O as measured by TGA (see FS3).

Figure 1 shows scanning electron microscopy (SEM) and transmission electron microscopy (TEM) images of the RG-O/Fe_2O_3 composite. The low-magnification image in Figure 1a shows a curled morphology, consisting of a thin wrinkled "paperlike" structure. A higher magnification SEM image (Figure 1b) shows that the Fe_2O_3 nanoparticles are uniformly distributed on the surface of RG-O. The typical Fe_2O_3 particle size is ~60 nm in diameter, which can be further confirmed by the TEM image in Figure 1c. The high-resolution TEM image in Figure 1d shows the interface between RG-O and Fe_2O_3 particles. The lattice fringes having an interlayer distance of 0.25 nm agrees well with the spacing between (110) planes of Fe_2O_3 crystals.

To measure the performance of the RG-O/Fe_2O_3 composite as an anode for Li^+ batteries, the composite was mixed with polytetrafluoroethylene (PTFE) in a weight ratio of 95:5 for preparing a working electrode, which is equivalent to Fe_2O_3:RG-O:PTFE = 76:19:5 and is practical for commercial battery anodes. Carbon black or other carbonaceous materials were not added to the electrode, in contrast to other studies.[16,18,22] Conductive fillers lower the specific capacity of the electrode. Electrochemical measurements were carried out using 2032 coin cells with the as-prepared RG-O/Fe_2O_3

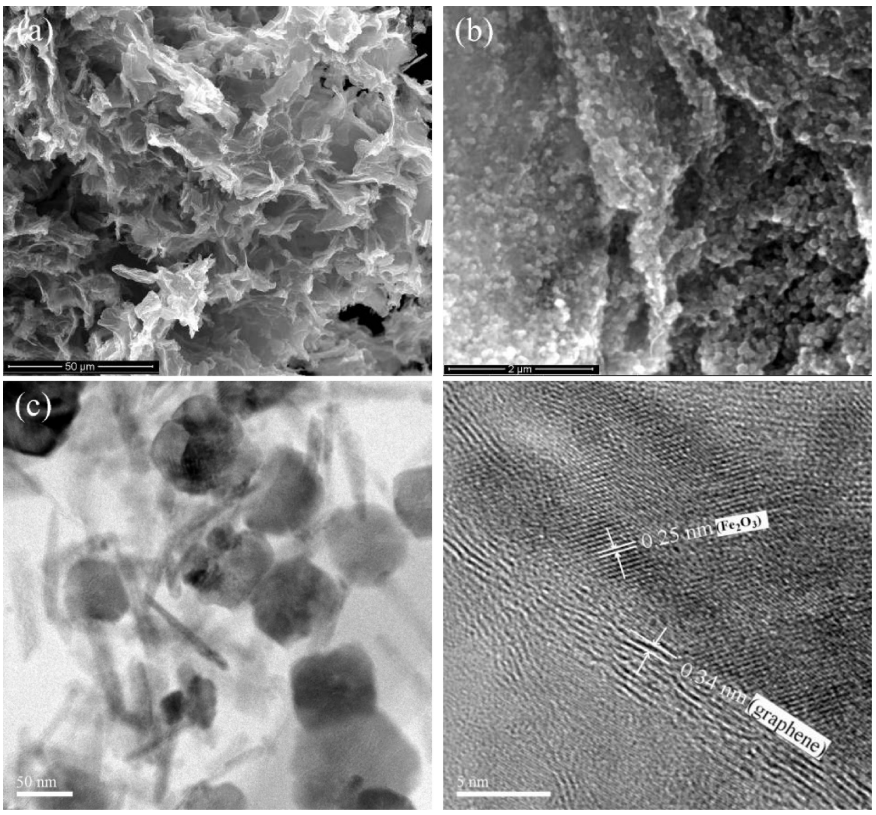

Figure 1. SEM and TEM images of the RG-O/Fe_2O_3 composite.

working electrode, lithium foil as the counter electrode, and 1 M $LiPF_6$ in ethylene carbonate (EC)/diethyl carbonate (DEC) (1:1 by volume) as the electrolyte.

Figure 2a shows the initial discharge and charge curves of the RG-O/Fe_2O_3 composite at a current density of 100 mA/g and a voltage range between 3.0 and 0.005 V vs Li^+/Li. In the discharge curve of the first cycle there are two obvious voltage plateaus (~1.6 and ~0.8 V vs Li^+/Li), resulting from the lithium reaction with Fe_2O_3 nanoparticles.[11,23] The voltage plateau at ~1.6 V has been reported in nanoscale hematite particles and is ascribed to Li insertion into the Fe_2O_3 structure,[24] and the plateau at ~0.80 V reflects the reduction of Fe(III) to Fe(0). The charge curve showed a sloping plateau at ~2.0 V due to the reverse reaction. It can be seen that the first discharge and charge capacities are 1693 (equivalent to 10.1 Li per Fe_2O_3 mole) and 1227 mAh/g (equivalent to 7.3 Li per Fe_2O_3 mole), respectively, based on the mass of Fe_2O_3 in the composite (the values are ~1355 and 982 mAh/g, respectively, based on the total mass of the RG-O/Fe_2O_3 composite).

For the complete reduction of $Fe^{3+} \rightarrow Fe^0$, one would expect a maximum uptake of 6 Li/Fe_2O_3 (~1005 mAh/g).[11] The excess capacity appears to derive from electrolyte decomposition in the low-potential region and the subsequent formation of an organic layer on the surface of the particles,[25,26] as well as Li insertion/extraction (or, simply, decoration on open surfaces) of RG-O platelets. The Li insertion/extraction/decoration in RG-O may play a major role in the overall electrochemical process and could be the reason for the excess capacity of the RG-O/Fe_2O_3 composite electrode. In the first discharge profile, the voltage plateau is longer, and correspondingly the total first-discharge capacity of 10.1 mol of Li is also larger than the 8.8 Li observed by Larcher *et al.*[27] and Chen *et al.*[23] and 8.3 mol of Li reported by Mores *et al.*[24] The plateau voltage at 0.8 V can also contain the Li insertion voltage plateau of RG-O (see FS4). The results indicate that the RG-O/Fe_2O_3 composite has more lithium insertion/extraction sites because the Fe_2O_3 nanoparticles anchor on the surface of the RGO sheets and act as spacers between RGO sheets, leading to higher discharge and charge capacities.

Figure 2b shows the cycle performance of the RG-O/Fe_2O_3 composite at 100 mA/g in the range between 3.0 and 0.005 V. The discharge capacities of the electrode in the first, 10th, 20th, 30th, and 50th cycle are 1693, 1142, 1120, 1098, and 1027 mAh/g, respectively, indicating that the RG-O/Fe_2O_3 composite electrode has a much higher capacity than graphite as well as good capacity retention. The RG-O/Fe_2O_3 composite showed good rate performance as well (Figure 2c). The capacity was as high as ~800 mAh/g even at a current density of 800 mA/g (see FS5).

The high capacity, good cycling stability, and rate capability of the RG-O/Fe_2O_3 composite anode materials are attributed to the intimate interaction between Fe_2O_3 nanoparticles and RG-O platelets. Because Fe_2O_3

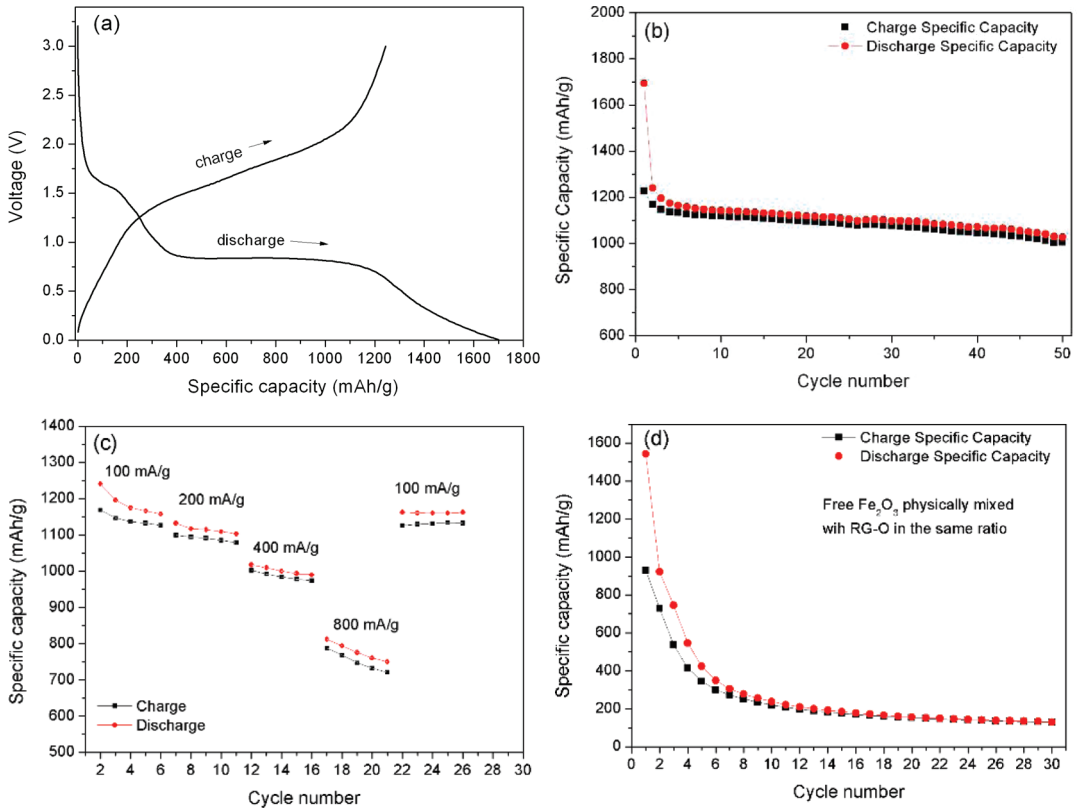

Figure 2. Electrochemical performance of the RG-O/Fe_2O_3 composite. The specific capacities are based on the mass of Fe_2O_3 in the RG-O/Fe_2O_3 composite. (a) Discharge/charge profiles of RG-O/Fe_2O_3 composite for the first cycle at the current density of 100 mA/g. (b) Cycling performance of RG-O/Fe_2O_3 composite at the current density of 100 mA/g. (c) Rate capacity of RG-O/Fe_2O_3 composite between 0.005 and 3.0 V with increasing current density. (d) Capacity retention of free Fe_2O_3 nanoparticles physically mixed with RG-O platelets at a current density of 100 mA/g.

nanoparticles anchored on the surface of RG-O platelets act as spacers between these platelets, the composite could provide more electrochemically active insertion/extraction lithium sites for the Fe_2O_3 nanoparticles as well as insertion/extraction/decoration sites from the highly conducting three-dimensional RG-O platelet network. In this composite, RG-O not only acts as a conductive additive but also offers sites for lithium insertion/desertion during charge and discharge. The electrochemical reaction mechanism of Li with Fe_2O_3 in Li-ion batteries can be described as

$$Fe_2O_3 + 6Li^+ + 6e^- \rightleftharpoons 2Fe + 3Li_2O$$

Fe_2O_3 can have an uptake of 6 Li, corresponding to 1005 mAh/g theoretical specific capacity. On the other hand, lithium can also be inserted/extracted ("decorated") on both sides of the RG-O platelets. The uniform mixture and interaction of Fe_2O_3 nanoparticles and RG-O platelets prevents both the aggregation of Fe_2O_3 nanoparticles and the restacking of RG-O sheets, which likely enhances cycle stability.

For comparison, we synthesized free Fe_2O_3 without any RG-O using the same homogeneous precipitation under microwave irradiation. The morphology of free Fe_2O_3 is similar to those of Fe_2O_3 nanoparticles in the composite in terms of size and crystallinity. The electrochemical performance was tested for the free Fe_2O_3 nanoparticles physically mixed with as-prepared RG-O in the relative weight ratio. At a current of 100 mA/g, the free Fe_2O_3 nanoparticles showed initial discharge and charge capacities of 1542 and 930 mAh/g, respectively, which further decreased to 130 and 129 mAh/g, respectively, after 30 cycles (Figure 2d). The comparison of the first cycle among RG-O, free Fe_2O_3, and the RG-O/Fe_2O_3 composite (FS4) shows that the total specific capacity of the RG-O/Fe_2O_3 composite is higher than the sum of free Fe_2O_3 and RG-O in their mass-weighted ratios. This indicates a positive synergistic effect of RG-O platelets and Fe_2O_3 nanoparticles in the composite prepared with urea followed by microwave curing in the presence of hydrazine, for improved electrochemical performance.

CONCLUSIONS

In summary, we report a simple two-step process to fabricate RG-O platelet/Fe_2O_3 nanoparticle composite as a high-performance anode material for Li-ion batteries. The composite exhibits 1693 and 1227 mAh/g for the first discharge and charge capacities, respectively, at a current density of 100 mAh/g. It shows a good capacity retention with 1027 mAh/g after the 50th discharge, as well as ~800 mAh/g of discharge

capacity even at the current density of 800 mA/g (based on the mass of Fe_2O_3 in the composite). The total specific capacity of RG-O/Fe_2O_3 is higher than the sum of pure RG-O and nanoparticle Fe_2O_3, indicating a positive synergistic effect of RG-O and Fe_2O_3 on the improvement of electrochemical performance. Our simple synthesis method can be readily adapted to prepare other high-performance anodes and cathodes containing "graphene" as a conducting additive that also binds Li further to enhance capacity.

METHODS

Synthesis of Graphite Oxide. Graphite oxide was synthesized from natural graphite by a modified Hummers method.[19,20] Briefly, graphite powder (2 g; SP-1, Bay Carbon, MI) and $NaNO_3$ (1 g; Aldrich, >99%) were mixed, then put into concentrated H_2SO_4 (96 mL; Fisher Scientific, 98%) with an ice bath. Under vigorous stirring, $KMnO_4$ (6 g; Fisher Scientific, 99.6%) was added gradually, and the temperature of the mixture was kept below 20 °C. After removing the ice bath, the mixture was stirred at 35 °C in a water bath for 18 h. As the reaction progressed, the mixture became pasty with a brownish color. Successively, 150 mL of H_2O was slowly added to the pasty mixture. Addition of water into the concentrated H_2SO_4 medium will release a large amount of heat; therefore, water should be added while keeping the mixture in an ice bath to keep the temperature below 50 °C. After dilution with 240 mL of H_2O, 5 mL of 30% H_2O_2 (Fisher Scientific) was added to the mixture, and the diluted solution color changed to brilliant yellow along with bubbling. After continuously stirring for 2 h, the mixture was filtered and washed with 10% HCl aqueous solution (250 mL; Fisher Scientific), DI water, and ethanol (Fisher Scientific, anhydrous) to remove other ions.[28] Finally, the resulting solid was dried by vacuum.

Prepararion of RG-O/Fe_2O_3 Composite. The RG-O/Fe_2O_3 composite was prepared by homogeneous precipitation and then subsequent reduction with hydrazine under microwave irradiation. In a typical experiment, 5 mmol of $FeCl_3$ (0.81 g; Aldrich, 98%) was dissolved in 50 mL of water, 150 mmol of urea (9.0 g; Aldrich, 98%) was separately dissolved in 50 mL of water, and then urea and $FeCl_3$ solutions were slowly and sequentially added to 50 mL of 2 mg/mL graphite oxide suspension under stirring. After exposure to ultrasound from an ultrasonic bath (VWR, B2500A-MT) for 30 min, the mixture was heated at 90 °C for 1.5 h. When cooled to room temperature, 0.5 mL of N_2H_4 (Aldrich, 64−65%) was added to the mixture while it was stirred. Then the mixture was put in a microwave oven (Sensor Microwave Oven, DE68-00307A) and irradiated for 2 min, in which time the mixture color changed from black-brown to black. Then, the black mixture was collected by filtration. After washing with DI water in an attempt to remove any excess hydrazine as well as other ions, the RG-O/Fe_2O_3 composite was obtained by drying at 80 °C for 24 h under vacuum.

Characterization. The structure of the obtained RG-O/Fe_2O_3 composite was characterized by X-ray diffraction (XRD) (pert, Philips) using Cu Kα radiation. SEM investigations were performed using an FEI Quanta-600 FEG Environmental SEM. HRTEM (JEOL 2010F TEM, 200 keV, 151−154 mA, spot size 1) was used to study the morphology and microstructure of the composites. Micro-Raman measurements of the samples were carried out using a WiTec Alpha300 system with a 532 nm wavelength incident laser light. Thermogravimetric analysis (TGA) was measured with a Perkin-Elmer TGA 4000 with a heating rate of 5 °C/min under 20 mL/min of flowing air. X-ray photoelectron spectroscopy (XPS) analysis was performed using a Kratos AXIS Ultra DLD XPS equipped with a 180° hemispherical energy analyzer to characterize the particles' surface. Photoemission was stimulated by monochromated Al Kα radiation (1486.6 eV) with an operating power of 150 W. It was operated in the analyzer mode at 80 eV for survey scans and 20 eV for detailed scans of core level lines. Binding energies were referenced to the C 1s binding energy set at 284.5 eV.

Electrochemical Characterization. Electrochemical experiments were performed using 2032 coin-type cells. The working electrode consisted of 95 wt % active material and 5 wt % polytetrafluoroethylene binder. The electrolyte was a solution of 1 M $LiPF_6$ in EC/DEC (1:1 by volume) (purchased from Novolyte). Pure Li foil (Aldrich) was used as the counter electrode. Celgard 2300 was used as a separator. The cells were discharged and charged galvanostatically in the voltage window from 0.005 to 3.0 V using a Land battery tester (China) at room temperature.

Acknowledgment. This work was supported by The University of Texas at Austin, the U.S. Department of Energy, Office of Basic Energy Sciences, Division of Materials Sciences and Engineering under Award DE-SC001951, the National Science Foundation (DMR-0907324), the China Scholarship Council Fellowship, and the Project sponsored by SRF for ROCS, SEM.

Supporting Information Available: Supplementary XRD, XPS, Raman spectrum, TGA, and additional electrochemical performance figures. This material is available free of charge *via* the Internet at http://pubs.acs.org.

Note Added after ASAP Publication: After this paper was published online March 31, 2011, a correction was made to the Acknowledgment. The revised version was published April 26, 2011.

REFERENCES AND NOTES

1. Buqa, H.; Goers, D.; Holzapfel, M.; Spahr, M. E.; Novak, P. High Rate Capability of Graphite Negative Electrodes for Lithium-Ion Batteries. *J. Electrochem. Soc.* **2005,** *152*, A474–A481.
2. Taberna, P. L.; Mitra, S.; Poizot, P.; Simon, P.; Tarascon, J. M. High Rate Capabilities Fe_3O_4-Based Cu Nano-Architectured Electrodes for Lithium-Ion Battery Applications. *Nat. Mater.* **2006,** *5*, 567–573.
3. Poizot, P.; Laruelle, S.; Grugeon, S.; Dupont, L.; Tarascon, J. M. Nano-Sized Transition-Metal Oxides as Negative-Electrode Materials for Lithium-Ion Batteries. *Nature* **2000,** *407*, 496–499.
4. Du, N.; Zhang, H.; Chen, B.; Wu, J. B.; Ma, X. Y.; Liu, Z. H.; Zhang, Y. Q.; Yang, D.; Huang, X. H.; Tu, J. P. Porous Co_3O_4 Nanotubes Derived From Co-4(CO)(12) Clusters on Carbon Nanotube Templates: A Highly Efficient Material for Li-Battery Applications. *Adv. Mater.* **2007,** *19*, 4505–4509.
5. Chernova, N. A.; Roppolo, M.; Dillon, A. C.; Whittingham, M. S. Layered Vanadium and Molybdenum Oxides: Batteries and Electrochromics. *J. Mater. Chem.* **2009,** *19*, 2526–2552.
6. Zhu, X. J.; Guo, Z. P.; Zhang, P.; Du, G. D.; Zeng, R.; Chen, Z. X.; Li, S.; Liu, H. K. Highly Porous Reticular Tin-Cobalt Oxide Composite Thin Film Anodes for Lithium Ion Batteries. *J. Mater. Chem.* **2009,** *19*, 8360–8365.
7. Lee, S. H.; Kim, Y. H.; Deshpande, R.; Parilla, P. A.; Whitney, E.; Gillaspie, D. T.; Jones, K. M.; Mahan, A. H.; Zhang, S. B.; Dillon, A. C. Reversible Lithium-Ion Insertion in Molybdenum Oxide Nanoparticles. *Adv. Mater.* **2008,** *20*, 3627–3632.
8. Arico, A. S.; Bruce, P.; Scrosati, B.; Tarascon, J. M.; Van Schalkwijk, W. Nanostructured Materials for Advanced Energy Conversion and Storage Devices. *Nat. Mater.* **2005,** *4*, 366–377.

9. Pushparaj, V. L.; Shaijumon, M. M.; Kumar, A.; Murugesan, S.; Ci, L.; Vajtai, R.; Linhardt, R. J.; Nalamasu, O.; Ajayan, P. M. Flexible Energy Storage Devices Based on Nanocomposite Paper. *Proc. Natl. Acad. Sci. U. S. A.* **2007,** *104*, 13574–13577.
10. Reddy, M. V.; Yu, T.; Sow, C. H.; Shen, Z. X.; Lim, C. T.; Rao, G. V. S.; Chowdari, B. V. R. Alpha-Fe_2O_3 Nanoflakes as an Anode Material for Li-Ion Batteries. *Adv. Funct. Mater.* **2007,** *17*, 2792–2799.
11. Larcher, D.; Masquelier, C.; Bonnin, D.; Chabre, Y.; Masson, V.; Leriche, J. B.; Tarascon, J. M. Effect of Particle Size on Lithium Intercalation into Alpha-Fe_2O_3. *J. Electrochem. Soc.* **2003,** *150*, A133–A139.
12. Stankovich, S.; Dikin, D. A.; Dommett, G. H. B.; Kohlhaas, K. M.; Zimney, E. J.; Stach, E. A.; Piner, R. D.; Nguyen, S. T.; Ruoff, R. S. Graphene-Based Composite Materials. *Nature* **2006,** *442*, 282–286.
13. Miller, J. R.; Outlaw, R. A.; Holloway, B. C. Graphene Double-Layer Capacitor with Ac Line-Filtering Performance. *Science* **2010,** *329*, 1637–1639.
14. Li, X. S.; Cai, W. W.; An, J. H.; Kim, S.; Nah, J.; Yang, D. X.; Piner, R.; Velamakanni, A.; Jung, I.; Tutuc, E.; *et al*. Large-Area Synthesis of High-Quality and Uniform Graphene Films on Copper Foils. *Science* **2009,** *324*, 1312–1314.
15. Geim, A. K. Graphene: Status and Prospects. *Science* **2009,** *324*, 1530–1534.
16. Wang, H.; Cui, L.-F.; Yang, Y.; Sanchez Casalongue, H.; Robinson, J. T.; Liang, Y.; Cui, Y.; Dai, H. Mn_3O_4-Graphene Hybrid as a High-Capacity Anode Material for Lithium Ion Batteries. *J. Am. Chem. Soc.* **2010,** *132*, 13978–13980.
17. Wang, D. H.; Choi, D. W.; Li, J.; Yang, Z. G.; Nie, Z. M.; Kou, R.; Hu, D. H.; Wang, C. M.; Saraf, L. V.; Zhang, J. G.; *et al*. Self-Assembled TiO_2-Graphene Hybrid Nanostructures for Enhanced Li-Ion Insertion. *ACS Nano* **2009,** *3*, 907–914.
18. Paek, S. M.; Yoo, E.; Honma, I. Enhanced Cyclic Performance and Lithium Storage Capacity of SnO_2/Graphene Nanoporous Electrodes with Three-Dimensionally Delaminated Flexible Structure. *Nano Lett.* **2009,** *9*, 72–75.
19. Hummers, W. S.; Offeman, R. E. Preparation of Graphitic Oxide. *J. Am. Chem. Soc.* **1958,** *80*, 1339–1339.
20. Stankovich, S.; Piner, R. D.; Nguyen, S. T.; Ruoff, R. S. Synthesis and Exfoliation of Isocyanate-Treated Graphene Oxide Nanoplatelets. *Carbon* **2006,** *44*, 3342–3347.
21. Lu, J.; Jiao, X.; Chen, D.; Li, W. Solvothermal Synthesis and Characterization of Fe_3O_4 and γ-Fe_2O_3 Nanoplates. *J. Phys. Chem. C* **2009,** *113*, 4012–4017.
22. Zhou, G. M.; Wang, D. W.; Li, F.; Zhang, L. L.; Li, N.; Wu, Z. S.; Wen, L.; Lu, G. Q.; Cheng, H. M. Graphene-Wrapped Fe_3O_4 Anode Material with Improved Reversible Capacity and Cyclic Stability for Lithium Ion Batteries. *Chem. Mater.* **2010,** *22*, 5306–5313.
23. Chen, J.; Xu, L. N.; Li, W. Y.; Gou, X. L. Alpha-Fe_2O_3 Nanotubes in Gas Sensor and Lithium-Ion Battery Applications. *Adv. Mater.* **2005,** *17*, 582–590.
24. Morales, J.; Sanchez, L.; Martin, F.; Berry, F.; Ren, X. L. Synthesis and Characterization of Nanometric Iron and Iron-Titanium Oxides by Mechanical Milling: Electrochemical Properties as Anodic Materials in Lithium Cells. *J. Electrochem. Soc.* **2005,** *152*, A1748–A1754.
25. Xing, W. B.; Dahn, J. R. Study of Irreversible Capacities for Li Insertion in Hard and Graphitic Carbons. *J. Electrochem. Soc.* **1997,** *144*, 1195–1201.
26. Mukai, S. R.; Hasegawa, T.; Takagi, M.; Tamon, H. Reduction of Irreversible Capacities of Amorphous Carbon Materials for Lithium Ion Battery Anodes by Li_2CO_3 Addition. *Carbon* **2004,** *42*, 837–842.
27. Larcher, D.; Bonnin, D.; Cortes, R.; Rivals, I.; Personnaz, L.; Tarascon, J. M. Combined XRD, EXAFS, and Mossbauer Studies of the Reduction by Lithium of Alpha-Fe_2O_3 with Various Particle Sizes. *J. Electrochem. Soc.* **2003,** *150*, A1643–A1650.
28. Kim, F.; Luo, J. Y.; Cruz-Silva, R.; Cote, L. J.; Sohn, K.; Huang, J. X. Self-Propagating Domino-Like Reactions in Oxidized Graphite. *Adv. Funct. Mater.* **2010,** *20*, 2867–2873.